

## Giant magnetothermal conductivity in the Ni–Mn–In ferromagnetic shape memory alloys

B. Zhang and X. X. Zhang<sup>a)</sup>

*Department of Physics and Institute of Nanoscience and Technology, The Hong Kong University of Science and Technology, Clear Water Bay, Kowloon, Hong Kong, People's Republic of China*

S. Y. Yu, J. L. Chen, Z. X. Cao, and G. H. Wu<sup>b)</sup>

*Beijing National Laboratory for Condensed Matter Physics, Institute of Physics, Chinese Academy of Sciences, Beijing 100080, People's Republic of China*

(Received 15 March 2007; accepted 8 June 2007; published online 6 July 2007)

In this letter the authors present the observation of giant magnetothermal conductivity in NiMnIn single crystals. Upon cooling, a martensitic transformation is accompanied by a ferromagnetic metal  $\rightarrow$  ferrimagnetic poor-metal transition. Most strikingly, this transition can be shifted to lower temperature and even totally suppressed by a magnetic field. The magnetic field-induced phase transition leads to a large magnetoresistance and a large magnetothermal conductivity up to 70% and 120%, respectively. The specific heat measurements indicate that the large magnetotransport properties are due to the increasing the density of free electrons, suggesting existence of superzone gap in the low-temperature, ferrimagnetic martensite. © 2007 American Institute of Physics. [DOI: 10.1063/1.2753710]

Very recently, Kainuma *et al.* discovered magnetic-field-induced shape recovery by reverse phase transformation in NiCoMnIn single crystals.<sup>1</sup> Most interestingly, the transformation from ferromagnetic parent phase to antiferromagnetic (or paramagnetic) martensitic phase was also shifted downward about 30 K. These results are totally different from that in other typical Heusler alloys, such as Ni<sub>2</sub>MnGa, where the magnetic field has a little or no influence on the transformation temperature.<sup>2–6</sup> The field-induced phase transition and the magnetic properties of NiMnIn alloys have then been intensively studied.<sup>7–10</sup> It is well known that colossal magnetoresistance (CMR) in the Mn-based perovskites is closely related to a magnetic field-induced magnetostructural phase transition.<sup>11,12</sup> In addition to CMR, many other interesting physical phenomena, e.g., magnetothermal properties,<sup>13–16</sup> were observed during the field-induced phase transition in these materials. Indeed, we have observed a large MR (>80%) in a wide temperature range in the NiMnIn single crystals.<sup>17</sup> Therefore, it is interesting and essential to investigate the origin of the large MR. To achieve this, the temperature and field-dependent magnetization, electrical resistivity, thermal conductivity, and specific heat measurement have been performed. Giant magnetothermal conductivity was observed in a wide temperature range. The observed large MR and giant magnetothermal conductivity can be ascribed to the collapsing of the “superzone gap,” as observed in intermetallic alloys at the order-disorder phase transition.<sup>18–20</sup> Superzone gap arises from the fact that the antiferromagnetic lattice does not commensurate with the crystal lattice, which leads to creation of new Brillouin boundary (a gap appearing on the Fermi surface).<sup>19</sup>

High quality Ni<sub>50</sub>Mn<sub>50–x</sub>In<sub>x</sub> ( $x=14–16.3$ ) single crystals were grown at a rate of 5–30 mm/h using a Czochralski method with a cold crucible system. High-temperature phase is L21-type ordered structure with a lattice constant  $a$

$=6.006 \text{ \AA}$ . Cooling to 93 K, the crystal structure changes to an orthorhombic structure with a rather complex martensitic modulated substructure. The magnetic properties, (magneto) transport properties, and heat capacity of the crystals were measured using a Quantum Design superconducting quantum interference device magnetometer (MPMS-5a) and a Quantum Design physical properties measurement system (PPMS-9).

Figure 1 shows the isofield  $M_B(T)$  magnetization, isofield  $\rho_B(T)$  electrical resistivity, and thermal conductivity curves of Ni<sub>50</sub>Mn<sub>33.7</sub>In<sub>16.3</sub> crystal measured in ZFC-FC process. The FC magnetization curve in 0.01 T field exhibits clearly two phase transitions at 315 and 130 K (the temperatures of middle transition), respectively. The thermal hysteresis around transition at 130 K is apparently due to the first-order, martensitic transition. The sharp drop in the ZFC-FC magnetization curves at 315 K is totally reversible, indicating that this transition is second order in nature and the Curie temperature ( $T_C$ ) of the austenite is 315 K. The most striking feature of the zero-field  $\rho(T)$  is that it rises sharply more than two times in magnitude at the phase transition, and then is weakly temperature independent below the transition. This metal/poor-metal transition must be caused by the first-order structural and magnetic phase transition. A thermal hysteresis appeared also in  $\rho(T)$  curves at the same temperature range as observed in low-field  $M_B(T)$  curves. This metal/poor-metal transition at martensitic transformation is very rare and interesting in ferromagnetic (FM) Heusler alloys because both the martensite and austenite in most Heusler alloys are metallic and exhibit similar  $\rho(T)$  behavior.<sup>5,6</sup> Therefore, this unique metal/poor-metal transition must be a consequence of a change in electronic band structure caused by the structural and magnetic phase transition. One possibility may be the establishment of a gap at the Fermi surface due to the “superzone effect” as observed in intermetallic alloys at the order-disorder phase transition.<sup>18–20</sup>

Several features in Fig. 1 are very striking in comparison with that observed in previous FM Heusler alloys, e.g.,

<sup>a)</sup>Electronic mail: phxxz@ust.hk

<sup>b)</sup>Electronic mail: ghwu@aphy.iphy.ac.cn

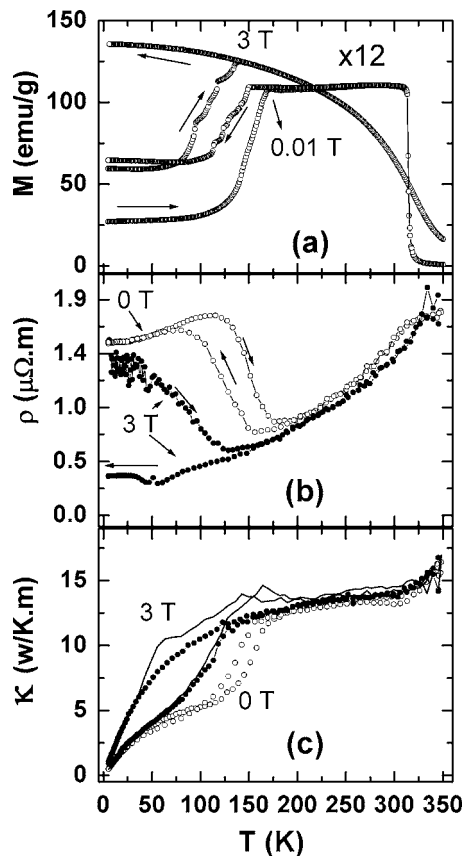


FIG. 1. Temperature-dependent magnetization (a) resistivity (b) and thermal conductivity (c) for  $\text{Ni}_{50}\text{Mn}_{33.7}\text{In}_{16.3}$  single crystal. The curves were measured by cycling temperature from 5  $\rightarrow$  350  $\rightarrow$  5 K in different magnetic fields after cooling the sample at a zero field to 5 K.

$\text{Ni}_2\text{MnGa}$  single crystals. (1) The low-temperature martensite is a poor-metallic ferrimagnet and high-temperature austenite is a metallic ferromagnet; (2) there is a very big magnetization difference between the two phases even under a 3 T magnetic field; (3) the phase transition can be significantly shifted to lower temperatures by an external magnetic field upon cooling, and even totally suppressed; (4) a large magnetoresistance,  $\text{MR} = -[\rho(3\text{ T}) - \rho(0)]/\rho(0)$  as large as 70% appears in a very wide temperature range of 5–100 K, which is slightly smaller than that observed in  $\text{Ni}_{50}\text{Mn}_{33.7}\text{In}_{16.3}$  single crystal.<sup>17,21</sup> This MR is very different from the CMR observed in the Mn-based perovskites and MnAs alloys, where the magnetic field shifts the low-temperature metal  $\rightarrow$  high-temperature insulator transition to higher temperatures.<sup>11,12,22</sup>

The strongly field-dependent martensitic transition temperature  $T_M$  in  $\text{NiMnIn}$  may be understood with the Clausius-Clapeyron relation, as discussed previously.<sup>1,17</sup> The poor-metal behavior of the martensite in  $\text{NiMnIn}$  should not be due to the scattering of the increased twin boundaries in the martensite because twin boundaries appear in all the martensitic phases of other Huesler alloys. Interestingly, in our  $\text{NiMnIn}$  alloys, the low-temperature martensite shows a much lower saturation magnetization than the austenite even under a very high field [Fig. 1(a)]. This may imply that the microscopic spin ordering in martensite is quite different from that in austenite. The field-induced phase transition will certainly change the fundamental ordering of spins and consequently the crystal structure,<sup>1,8,9,19</sup> which should give rise to a change in the electronic band structure.

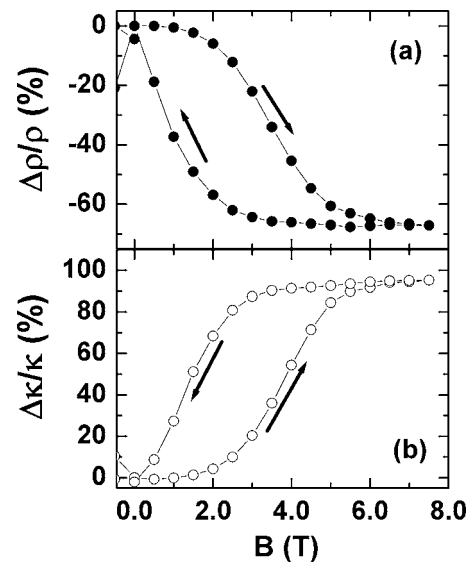


FIG. 2. Representative magnetic field-dependent magnetoresistance (a) and magnetothermal conductivity at 60 K for  $\text{Ni}_{50}\text{Mn}_{33.7}\text{In}_{16.3}$  single crystal.

If the metal/poor-metal transition at the martensitic transformation is due to the superzone effect of the ferrimagnetic ordering, the field-induced ferrimagnetic to ferromagnetic transition should lead to gap collapsing at the Fermi surface, consequently to an increase of the density of conducting electrons.<sup>18–20</sup> Antiferromagnetic ordering (or phase) was observed in Mn-doped  $\text{Ni}_2\text{MnGa}$  alloys, which support the ferrimagnetic ordering in  $\text{Ni}_{50}\text{Mn}_{50-x}\text{In}_x$  ( $x=14–16.3$ ) single crystals whose Mn content is much higher than 25% in  $\text{Ni}_2\text{MnGa}$ .<sup>23</sup>

If it is true, we should expect a large magnetothermal conductivity ( $\text{MTC} = [\kappa(H) - \kappa(0)]/\kappa(0)$ ) caused by the magnetic field-induced phase transition. In Fig. 1(c)  $\kappa(T)$  curves are shown. As expected, zero-field  $\kappa(T)$  decreases sharply at  $T_M$  upon cooling due to the reduction of the free electron density. The most striking feature in Fig. 1(c) is that when the martensitic transformation is suppressed by a 3 T field upon cooling,  $\kappa(T)$  is greatly enhanced. The MTC reaches about 120% at about 50 K, and is more than 70% in a 100 K temperature range. This MTC is much larger than that observed in perovskites,<sup>13–16</sup> and it should be the largest one observed in magnetic materials.

To correlate the MR and MTC, we calculated the increased electronic thermal conductivity  $\Delta\kappa_{\text{el}}$  using the electronic conductivity change ( $\Delta\sigma$ ) extracted from  $\rho(T)$  in Fig. 1(b) and the free electron Wiedemann-Franz law,  $k/\sigma T = L = 2.45 \times 10^{-8} \text{ W } \Omega \text{ K}^{-2}$ , which provides the upper bound for  $\Delta\kappa_{\text{el}}$ . The sum of  $\Delta\kappa_{\text{el}}$  and zero-field  $\kappa$  gives total  $\kappa$  [solid lines in Fig. 1(c)], which is in a good accordance with the measured thermal conductivity in 3 T field. In Fig. 2 the field-dependent magnetoresistance and magnetothermal conductivity below the martensitic phase transition are presented. Due to the field-induced-phase transition, the crystal gradually transformed from ferrimagnetic poor metal to the ferromagnetic metal, i.e., the resistivity decreases and thermal conductivity increases. Now, it is clear that the same physical mechanism is responsible for the MR and MTC.

To confirm the existence of energy gap in ferrimagnetic martensite, we performed the specific heat ( $c_p$ ) measurement in zero and 9 T fields for the same sample (Fig. 3). The zero-field measurement was carried out from 5 to 30 K after

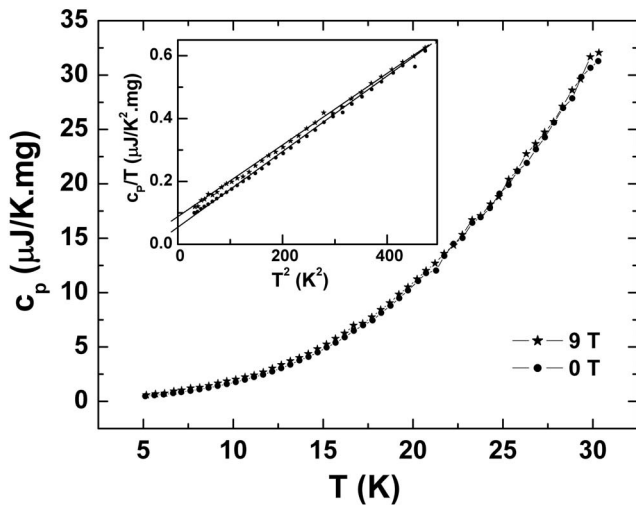


FIG. 3. Specific heat measured in magnetic fields of 0 and 9 T on  $\text{Ni}_{50}\text{Mn}_{34}\text{In}_{16.3}$  single crystal. The inset is the  $c_p/T$  against  $T^2$  for the low-temperature specific data, and the curve is the best linear fitting of the data.

zero-field cooled to 5 K, whereas the 9 T one was performed from 30 to 5 K after field-cooled from 300 K. The temperature-dependent magnetization and resistivity data (Fig. 1) measured in different magnetic fields show that the martensitic transition can be completely suppressed by a 3 T magnetic field upon cooling.<sup>21</sup> Therefore, the specific heat data measured with a 9 T magnetic field come from the ferromagnetic metal. Shown in the inset is the plot of  $c_p/T$  against  $T^2$  for the low-temperature data. By a linear fit, we obtained the values of  $\gamma$  in the expression of specific heat for a metallic crystal,  $c_p = \gamma T + AT^3$ , where  $\gamma T$  and  $AT^3$  are due to free electrons and lattice, respectively. The value of  $\gamma$  is given by

$$\gamma = V_m \left( \frac{1}{9\pi} \right)^{1/3} \left( \frac{k_B}{\hbar} \right)^2 m^* n^{1/3}, \quad (1)$$

where  $V_m$  is the molar volume,  $k_B$  is Boltzmann constant,  $\eta$  is the Planck constant divided by  $2\pi$ ,  $m^*$  is the electron effective mass, and  $n$  is the density of the free electrons. The value of  $\gamma$  is increased from  $0.054 \pm 0.001$  mJ/g K<sup>2</sup> for zero-field curve to  $0.085 \pm 0.001$  mJ/g K<sup>2</sup> for the 9 T curve, implying that the electronic contribution to the total specific heat is greatly increased when the material transforms from the ferrimagnetic to the ferromagnetic state. Based on the refined values of  $A$ , we found that Debye temperature ratio between the ferromagnetic and ferrimagnetic phases is about 0.97, indicating that phonon scatterings cannot lead to the huge increase of resistivity in ferrimagnetic phase. From Eq. (1), it is clear that the value of  $\gamma$  depends on both the effective mass and density of free electrons. If the enhanced  $\gamma$  is due to the increase in effective mass, the conductivity will decrease, which is contrary to the experimental results. Therefore, the enhanced  $\gamma$  should be due to the increase of the free electron density.<sup>18</sup> We estimated the increase of electron density using  $\gamma_9 T / \gamma_0 = (n_9 T / n_0)^{1/3}$  and found  $n_9 T / n_0 \approx 3.9$ . Consequently the MR value was estimated using this ratio and  $\rho = m / ne^2 \tau$  and

$$\text{MR} = [\rho(0) - \rho(9 \text{ T})] / \rho(0) = [1/n_0 - 1/n_9 T] n_0. \quad (2)$$

By assuming that the relaxation time  $\tau$  is the same for the ferromagnetic and ferrimagnetic phases, we obtained MR = 74.4%, being so close to the experimental data MR = 77.1% at 5 K.<sup>21</sup> We may conclude that great increase of the conduction electron density should be due to the collapse of the superzone gap by the field-induced ferrimagnetic to ferromagnetic phase transition.<sup>18–20</sup>

This work described in this letter is supported by grants from the Research Grants Council of the Hong Kong Special Administration Region and by CNSF, China.

- <sup>1</sup>R. Kainuma, Y. Imano, W. Ito, Y. Sutou, H. Morito, S. Okamoto, O. Kitakami, K. Oikawa, A. Fujita, T. Kanomata, and K. Ishida, *Nature (London)* **439**, 957 (2006).
- <sup>2</sup>K. Ullakko, J. K. Huang, C. Kantner, R. C. OHandley, and V. V. Kokorin, *Appl. Phys. Lett.* **69**, 1966 (1996); A. Sozinov, A. A. Likhachev, N. Lanska, and K. Ullakko, *ibid.* **80**, 1746 (2002).
- <sup>3</sup>G. H. Wu, C. H. Yu, L. Q. Meng, J. L. Chen, F. M. Yang, S. R. Qi, W. S. Zhan, Z. Wang, Y. F. Zheng, and L. C. Zhao, *Appl. Phys. Lett.* **75**, 2990 (1999).
- <sup>4</sup>K. Oikawa, L. Wulff, T. Iijima, F. Gejima, T. Ohmori, A. Fujita, K. Fukamichi, R. Kainuma, and K. Ishida, *Appl. Phys. Lett.* **79**, 3290 (2001).
- <sup>5</sup>F. Zuo, X. Su, and K. H. Wu, *Phys. Rev. B* **58**, 11127 (1998).
- <sup>6</sup>F. Zuo, X. Su, P. Zhang, G. C. Alexandrakakis, F. Yang, and K. H. Wu, *J. Phys.: Condens. Matter* **11**, 2821 (1999).
- <sup>7</sup>Y. Sutou, Y. Imano, N. Koeda, T. Omori, R. Kainuma, K. Ishida, and K. Oikawa, *Appl. Phys. Lett.* **85**, 4358 (2004).
- <sup>8</sup>K. Oikawa, W. Ito, Y. Imano, Y. Sutou, R. Kainuma, K. Ishida, S. Okamoto, O. Kitakami, and T. Kanomata, *Appl. Phys. Lett.* **88**, 122507 (2006).
- <sup>9</sup>R. Kainuma, Y. Imano, W. Ito, H. Morito, Y. Sutou, K. Oikawa, A. Fujita, K. Ishida, S. Okamoto, and O. Kitakami, *Appl. Phys. Lett.* **88**, 192513 (2006).
- <sup>10</sup>T. Krenke, E. Duman, M. Acet, E. F. Wassermann, X. Moya, L. Manosa, and A. Planes, *Nat. Mater.* **4**, 450 (2005); T. Krenke, M. Acet, E. F. Wassermann, X. Moya, L. Manosa, and A. Planes, *Phys. Rev. B* **73**, 174413 (2006).
- <sup>11</sup>R. Vonhelmolt, J. Wecker, B. Holzapfel, L. Schultz, and K. Samwer, *Phys. Rev. Lett.* **71**, 2331 (1993); S. Jin, T. H. Tiefel, M. McCormack, R. A. Fastnacht, R. Ramesh, and L. H. Chen, *Science* **264**, 413 (1994).
- <sup>12</sup>J. M. D. Coey, M. Viret, and S. von Molnar, *Adv. Phys.* **48**, 167 (1999); H. Kuwahara, Y. Tomioka, A. Asamitsu, Y. Moritomo, and Y. Tokura, *Science* **270**, 961 (1995).
- <sup>13</sup>D. W. Visser, A. P. Ramirez, and M. A. Subramanian, *Phys. Rev. Lett.* **78**, 3947 (1997).
- <sup>14</sup>B. X. Chen, J. H. Xu, C. Uher, D. T. Morelli, G. P. Meisner, J. P. Fleurial, T. Caillat, and A. Borschovsky, *Phys. Rev. B* **55**, 15471 (1997).
- <sup>15</sup>J. L. Cohn, J. J. Neumeier, C. P. Popoviciu, K. J. McClellan, and T. Leventouri, *Phys. Rev. B* **56**, R8495 (1997); M. Matsukawa, H. Ogasawara, R. Sato, M. Yoshizawa, R. Suryanarayanan, G. Dhalenne, A. Revcolevschi, and K. Itoh, *ibid.* **62**, 5327 (2000).
- <sup>16</sup>M. Matsukawa, H. Ogasawara, R. Sato, M. Yoshizawa, R. Suryanarayanan, G. Dhalenne, A. Revcolevschi, and K. Itoh, *Phys. Rev. B* **62**, 5327 (2000).
- <sup>17</sup>S. Y. Yu, Z. H. Liu, G. D. Liu, J. L. Chen, Z. X. Cao, G. H. Wu, B. Zhang, and X. X. Zhang, *Appl. Phys. Lett.* **89**, 162503 (2006).
- <sup>18</sup>N. V. Baranov, and E. A. Barabanova, *J. Alloys Compd.* **219**, 139 (1995); Y. Aoki, Y. Kobayashi, H. Sato, H. Sugawara, V. Sechovsky, L. Havela, K. Prokes, M. Mihalik, and A. Menovsky, *J. Phys. Soc. Jpn.* **65**, 3312 (1996).
- <sup>19</sup>V. Sechovsky, L. Havela, K. Prokes, H. Nakotte, F. R. Deboer, and E. Bruck, *J. Appl. Phys.* **76**, 6913 (1994).
- <sup>20</sup>V. N. Antonov, A. Y. Perlov, P. M. Oppeneer, A. N. Yaresko, and S. V. Halilov, *Phys. Rev. Lett.* **77**, 5253 (1996).
- <sup>21</sup>B. Zhang, X. X. Zhang, S. Y. Yu, J. L. Chen, and G. H. Wu (unpublished).
- <sup>22</sup>J. Mira, F. Rivadulla, J. Rivas, A. Fondado, T. Guidi, R. Caciuffo, F. Carsughi, P. G. Radaelli, and J. B. Goodenough, *Phys. Rev. Lett.* **90**, 097203 (2003).
- <sup>23</sup>J. Enkovaara, O. Heczko, A. Ayuela, and R. M. Nieminen, *Phys. Rev. B* **67**, 212405 (2003).